



Published in final edited form as:

Mol Pharm. 2013 January 7; 10(1): 26–32. doi:10.1021/mp300238w.

Endocytic uptake pathways utilized by CPMV nanoparticles

Emily M. Plummer^{1,2,#} and Marianne Manchester^{1,*}

¹Skaggs School of Pharmacy and Pharmaceutical Sciences, University of California, San Diego, La Jolla, CA 92093 USA

²Kellogg School of Science and Technology, The Scripps Research Institute, La Jolla, CA 92037 USA

Abstract

Cowpea mosaic virus (CPMV) has been used as a nanoparticle platform for biomedical applications including vaccine development, *in-vivo* vascular imaging, and tissue-targeted delivery. A better understanding of the mechanisms of CPMV targeting and cell internalization would enable enhanced targeting and more effective delivery. Previous studies showed that, following binding and internalization by mammalian cells, CPMV localizes in a perinuclear late-endosome compartment where it remains for as long as several days. To further investigate endocytic trafficking of CPMV within the cell, we used multiple approaches including pharmacologic inhibition of pathways, and co-localization with endocytic vesicle compartments. CPMV internalization was clathrin-independent, and utilized a combination of caveolar endocytosis and macropinocytosis pathways for entry. CPMV particles co-localized with Rab5⁺ early endosomes to traffic ultimately to a lysosomal compartment. These studies facilitate the further development of effective intracellular drug-delivery strategies using CPMV.

Keywords

Cowpea mosaic virus (CPMV); endocytosis; entry; caveolae; macropinocytosis; clathrin; Rab5; Rab11

Introduction

The unique properties of nanoparticles, including relatively large surface area, surface chemistry, and self-assembly, make these versatile platforms attractive for many applications. Biomedical applications are a major avenue of nanoparticle development, particularly disease diagnosis and targeted therapy^{1, 2}. To develop an effective platform for *in vivo* delivery, it is critical to understand not only how the formulation reaches tissues of interest, but also how formulations are internalized into cells and traffic within the cell to reach desired intracellular destinations. Such intracellular localization is essential to achieve maximum efficacy of targeted therapeutics.

The plant virus cowpea mosaic virus (CPMV) is one of many viral nanoparticles that are being developed as platforms for targeted delivery of therapies and imaging agents^{3–5}. CPMV is an attractive candidate because of several characteristics: excellent bioavailability

*Corresponding author: MC0749, 9500 Gilman Drive, La Jolla, CA 92093, mmanchester@ucsd.edu.

#Current address: La Jolla Institute for Allergy and Immunology, 9420 Athena Circle, La Jolla, CA 92037, Tel 858.752.6500

Supporting information: RAW264.7 macrophages were exposed to dynasore for 30 minutes prior to addition of CPMV. After 1 hour, cells were fixed and imaged by confocal microscopy. Levels of colocalization were determined using Image J. This information is available free of charge via the Internet at <http://pubs.acs.org/>.

and biocompatibility, low toxicity (where doses of at least 10^{16} particles/kg of body weight are tolerated), and wide biodistribution^{6, 7}. Previous studies have demonstrated the utility of CPMV-based formulations for intravital vascular imaging^{3, 8}, targeting to tumors³, targeting areas of inflammation in the central nervous system^{7, 9} and targeting atherosclerotic plaque in the cardiovascular system¹⁰.

The interaction of CPMV with vascular endothelial cells and macrophages is mediated by a surface form of the cytoskeletal protein vimentin^{11, 12}, a 54 kD protein that forms filamentous structures in the cytosol. Vimentin also has been found on the surface of several other cell types^{13–17}. After CPMV binds to surface vimentin and enters cells, at later time points (around 5h) CPMV particles colocalize with golgi (beta-COP marker) and late endosome compartments (Lamp-2 marker)³. However, the mechanism of entry, and the endocytic pathway taken by CPMV through the cell to reach these late compartments is unknown.

Nanoparticle therapeutics are being targeted to tumors using ligands such as antibodies, peptides or small-molecules¹⁸, that recognize markers that are differentially regulated or expressed in tumor compared to normal tissue^{19, 20}. Several challenging factors inhibit penetration of therapeutics into the tumor parenchyma, including increased interstitial pressures within the tumor, disorganized vascularization, and intratumoral architecture including interstitial spaces and non-tumor cells²¹. It is important to facilitate not only homing of a targeted therapeutic to the tumor, but delivery of the payload into the intracellular compartment where the therapeutic will have highest activity against the tumor and its microenvironment²². In general, the intracellular targeting of any class of nanoparticle has been studied only in a very limited way^{22–24}, and its relationship to drug efficacy is largely unknown^{22–25}.

Interestingly, viruses have long been the some of most informative molecular tools for defining fundamental cellular mechanisms of particle internalization and subcellular localization²⁶. A variety of studies of virus internalization have shown that following binding, potential mechanisms of internalization from the surface include entry via endosomes such as clathrin-coated pits or caveolae, macropinocytosis, as well as nontraditional routes of entry that do not involve clathrin-mediated or caveolar endocytosis (Figure 1). These pathways have been established using pharmacologic inhibitors of the respective pathways, or cell lines deficient or altered in essential components of the respective endocytic pathways²⁵. Markers of early, late, and recycling endosome compartments have also been established (Figure 1). In this study, the mechanism of CPMV entry in human HeLa epithelial carcinoma cells and murine RAW264.7 macrophages was characterized using small-molecule endocytosis inhibitors and known endocytic vesicle markers. CPMV entry and intracellular localization was studied using a combination of flow cytometry and fluorescence confocal microscopy.

Experimental Section

Cell Culture

RAW264.7 macrophages were grown and maintained in Dulbecco's minimum essential medium (DMEM) supplemented with 10% heat-inactivated fetal bovine serum albumin (FBS), 1% L-glutamine, and 1% penicillin/streptomycin. Hela cells were grown and maintained in Earle's minimum essential media (EMEM) supplemented with 10% heat-inactivated fetal bovine serum albumin (FBS), 1% L-glutamine, and 1% penicillin/streptomycin.

CPMV

Virus was grown in California Blackeye 5 seeds obtained from the Burpee Company (Warminster, PA). Plants were grown and mechanically inoculated with wild type CPMV and harvested 7–10 days later as described previously^{27, 28}. Virus purification and characterization was performed as described²⁹.

Surface modification of CPMV

To conjugate Alexa Fluor dyes (AF647 and AF488 carboxylic acid, succinimidyl ester, Molecular Probes Grand Island, NY) to addressable lysines present on the surface of wild-type CPMV, 1 mg of dye was resuspended in DMSO and combined with CPMV in 0.1 M K-phosphate buffer at a ratio of 2000 dye: 1 virus, in a total of 1 ml, with 90% buffer and 10% DMSO. The suspension was incubated on a rolling shaker for 24 hours at room temperature. The samples were purified by 3 hours ultracentrifugation at 42,000 rpm, followed by sucrose gradient (10%–30% w/v in phosphate buffer, 28,000 rpm for 3 hours) and a second ultracentrifugation spin. The pellet was resuspended in PBS and characterized by fluorescence spectroscopy and FPLC. The number of dyes per particle was calculated with the equation: $[(Abs_{495} \times dilution) / AlexaFluor\ dye] / (concentration\ of\ CPMV / molecular\ weight\ of\ CPMV)$; where the molecular weight of CPMV = 5.6×10^6 grams/mole.

General inhibition of CPMV uptake

To determine whether uptake of CPMV can be blocked using general inhibition, cells were incubated under varying metabolic conditions. In temperature studies, cells were incubated with 1×10^6 CPMV particles per cell at 37 °C for 4 hours, or 4 °C for 1 hour. To confirm whether nonspecific inhibitors could block endocytosis, cells were incubated in hypertonic sucrose (0.45 M sucrose, Fisher Scientific, Hampton, NH) or concanavalin A (250 µg/ml, St. Louis, MO) for 30 minutes prior to incubation with CPMV for 3 hours in the same conditions. Inhibitor activity was confirmed with the use of fluorescently labeled transferrin (clathrin-mediated endocytosis, Invitrogen, Grand Island, NY), cholera toxin (caveolae-mediated endocytosis, Invitrogen, Grand Island, NY), or 10,000 molecular weight dextran (macropinocytosis entry, 1 mg/ml Invitrogen, Grand Island, NY).

Clathrin-dependent endocytic pathway inhibition

To block clathrin-dependent endocytosis, cells were treated with 10 µM chlorpromazine (Invitrogen, Grand Island, NY) for 30 minutes. CPMV was then added at 1×10^6 particles/cell and incubated for 3 hours in the presence of chlorpromazine.

Caveolae-dependent endocytic pathway inhibition

Filipin III (Cayman Chemical Company, Ann Arbor, MI) and nystatin (Fisher Scientific, Hampton, NH), which deplete cholesterol, were used to inhibit caveolae-dependent endocytosis. Cells were preincubated for 30 minutes with 2 µg/ml filipin III or 20 µg/ml nystatin, before incubation with CPMV for 3 hours in the presence of inhibitors.

Dynamin-dependent pathway inhibition

Inhibition of dynamin, a protein that is involved in the pinching off of vesicles formed by both clathrin- and caveolae-dependent endocytosis, was studied using dynasore (EMD Millipore, Billerica, MA)³⁰. Cells were treated with 50 µM dynasore for 30 minutes prior to incubation with CPMV for 1 hour in the presence of inhibitor.

Macropinocytosis pathway inhibition

Amiloride or dimethylamiloride (30 μ M, MP Biomedicals, Solon, OH) were used to block macropinocytosis. Cells were pretreated with the inhibitor for 30 minutes before incubation with CPMV for 3 hours in the presence of inhibitors.

CPMV uptake into cells by flow cytometry

RAW264.7 macrophages and HeLa cells were removed from flasks using cell dissociation buffer and suspended in media in 96-well plates at 5×10^5 cells/well. Cells were treated with inhibitors for 30 minutes prior to addition of 100,000 dye-labeled CPMV particles per cell. After 3 hours, cells were washed and fixed in 4 percent EM grade formaldehyde. Data were collected at the UCSD VA Flow Cytometry core and analyzed using FlowJo (Tree Star Inc, Ashland, OR).

CPMV uptake into cells by confocal microscopy

Cells were initially grown to 80% confluency on glass-bottom confocal dishes (MatTek, Ashland, MA) before treatment, or a subset of treated cells were plated for the last hour of treatment on dishes. Cells were washed and fixed in 4 percent EM grade formaldehyde with 0.3% glutaraldehyde for 10 minutes. The cell membrane was stained prior to permeabilization using wheat germ agglutinin (WGA) directly conjugated to AF555 (Invitrogen, Grand Island NY). Cells were permeabilized and endosomal markers were stained using antibodies to EEA1 (Cell Signaling Technology, Beverly MA), LAMP-2 (Biolegend, San Diego CA), Rab11 (Cell Signaling Technology, Beverly MA) and Rab5 (BD Biosciences, San Jose CA). Images were collected on the Olympus FV1000 confocal microscope at the UCSD School of Medicine Light Microscopy Facility. Data was analyzed using ImageJ (<http://rsbweb.nih.gov/ij/>).

Results

In order to characterize the mechanism of endocytosis by CPMV, endocytosis inhibitors were used to perturb entry. Inhibitors that affect endocytic pathways in a more general manner, and inhibitors more specific to a particular pathway, were used to elucidate the pathways potentially involved in entry of CPMV. In addition, markers that are associated with particular endocytic vesicle compartments were imaged using antibodies and compared to localization of CPMV particles within the cell.

CPMV uptake in HeLa cells and RAW264.7 cells has been established in several studies^{10, 17, 31–33}. An example of CPMV binding and internalization by RAW264.7 macrophages using chemically-modified CPMV and confocal microscopy is shown in Figure 2. It has previously been shown that RAW264.7 macrophages display surface vimentin³³, a protein that has been shown to mediate entry of CPMV^{11, 12}. The addressable lysines on the surface of CPMV were labeled with AF647 or AF488, and the labeling density was approximately 80 fluorophores per particle. CPMV-AF647 conjugates were purified and incubated with RAW264.7 macrophages at 1×10^6 viruses per cell at 37 °C for 4 hours (internalization) or 4 degrees C for 1 hour (surface binding). In comparison to studies of virus entry using replication-competent viruses, a relatively high number of CPMV particles are needed to detect fluorescent virus particles because individual input virus particles are being detected, rather than amplification of viral protein expression following replication. In studies of virus-cell binding at 4°C, representative images showed fluorescence at the cell surface colocalized with the surface plasma membrane stain wheat germ agglutinin (WGA) in cells (Fig. 2A). In cells incubated for 4 hours at 37 °C to enable internalization, the AF647 fluorescence is visible inside the cell and in areas internal to the surface WGA staining (Fig. 2B). Previous studies showed that upon internalization of

CPMV, particles migrated to a perinuclear compartment by 5 hours post-incubation and remained there. In mouse bone marrow dendritic cells, the perinuclear compartment was shown to be endolysosomal by colocalization of particles with the markers LAMP-2 and beta-COP³. This phenomenon has also been observed in HeLa cells³². To determine if CPMV also traffics to the lysosomal compartment in RAW264.7 macrophages, cells were incubated with labeled CPMV for 5 hours at 37°C. Following fixation and permeabilization, cells were incubated with anti-lysosomal antibody LAMP-2 and incubated with a fluorescent secondary antibody. Cells were imaged by confocal microscopy and colocalization of CPMV fluorescence with the LAMP-2 marker in RAW264.7 macrophages was confirmed (Figure 2).

Pharmacologic inhibition of CPMV entry

In order to determine first whether CPMV entry could be inhibited, relatively nonspecific inhibitors that target multiple endocytic pathways were used. Cells were incubated with concanavalin A or with hypertonic sucrose for 30 minutes prior to addition of 1×10^5 particles/cell for 3 hours under endocytosis-inhibiting conditions (Figure 3A). For quantitative analysis by FACS, cells were processed at 5×10^5 cells per well in a 96-well plate. In order to remove particles bound to the cell surface but not internalized, cells were trypsinized prior to fixing and analysis, which has been previously shown to disrupt the CPMV-vimentin interaction and surface binding¹¹. Although concanavalin A was not as effective at reducing uptake (46%), hypertonic sucrose which inhibits endocytosis by clathrin-mediated, caveolar and macropinocytosis pathways³⁴ decreased the percentage of HeLa and RAW264.7 cells able to internalize CPMV by 98% and 85%, respectively (Figure 3A).

Specific endocytic pathways were first studied using dynasore (Figure 3A–C). The inhibitor dynasore blocks activity of dynamin, which is involved in the final stage of vesicle formation in both clathrin- and caveolae-mediated endocytosis. The application of dynasore 30 minutes prior to CPMV incubation reduced CPMV entry by 68% (HeLa) and 58% (RAW264.7 macrophages) (Figure 3A). Accumulation of CPMV at the surface of RAW264.7 macrophages was also increased from 57% in normal conditions to 78% under dynamin-inhibiting conditions, as determined by ImageJ analysis of colocalization of CPMV signal with plasma membrane stain (Figure 3B–C, Figure S1).

Next, inhibitors of clathrin-mediated endocytosis were used to determine the role of clathrin-coated pits in CPMV entry. The clathrin inhibitor chlorpromazine is a cationic amphipathic drug that relocates clathrin and adaptor protein complex-2 from the plasma membrane to the endosomal membrane³⁵. Chlorpromazine reduced uptake of CPMV by 11% (Figure 3A).

The lipid raft inhibitors nystatin and filipin III are used to block endocytosis that is mediated by caveolae. Treatment of HeLa cells with nystatin and filipin reduced internalization of CPMV by 27% and 48%, respectively. Filipin III was less effective at reducing uptake in RAW264.7 macrophages, causing only an 11% reduction in uptake. These results suggest that caveolae are likely involved in CPMV internalization (Figure 3A).

Amilorides are Na⁺/H⁺ exchange inhibitors that block macropinocytosis³⁶. In HeLa cells, amiloride treatment resulted in 30% reduced uptake of CPMV by FACS (Figure 3A). In addition, CPMV and dextran-FITC, which enters cells by macropinocytosis, showed colocalization by confocal microscopy, further suggesting a role for macropinocytosis in CPMV entry (Figure 3 D–E). Together these studies suggest that a combination of pathways is used for CPMV internalization, including caveolae and macropinocytosis.

Association of CPMV with early and recycling endosomal compartments

To further determine the role of endocytic pathways and vesicle compartments in CPMV entry, the endosomal markers EEA1, Rab 11 and Rab5, were investigated. Colocalization at early times post-entry with the endosomal marker EEA1 often correlates with entry by clathrin-mediated endocytosis, as EEA1 typically does not co-localize with caveosomes^{37, 38} (Figure 1). Rab5 is also an early endosomal marker that is associated with both clathrin-mediated and caveolar endocytosis. Endocytic vesicles of the recycling endosomal pathway can be identified by the presence of Rab11 on the vesicle surface. (Figure 1). HeLa cells were incubated with CPMV for different times, fixed, and stained with EEA1 antibody. Lack of colocalization with EEA1 at early timepoints (Figure 4 A–B), together with the relatively minor inhibition in uptake during chlorpromazine inhibition shown in Figure 3, further suggests that clathrin-mediated endocytosis is not significantly utilized by CPMV.

To study co-localization with Rab5, after 15, 30, 45, and 60 minutes of exposure to dye-labeled CPMV, cells were fixed and stained with Rab5 antibody. Partial colocalization of CPMV with the Rab5 marker was observed, particularly at 45 minutes after addition of CPMV (Figure 4C). Recycling endosomes were then identified using an anti-Rab11 antibody followed by a corresponding fluorescent secondary antibody. CPMV fluorescence was found to partially colocalize with the Rab11 antibody signal, particularly at later 1h and 3h timepoints (Figure 4D). Together these studies indicate that CPMV bypasses the EEA1 endosomal compartment and traffics through Rab5+ endosomes before accumulating in Lamp1+ late endolysosomes.

Discussion

Here the endocytic pathway of CPMV in HeLa and RAW264.7 macrophages was characterized. The clathrin-mediated endocytic pathway had limited involvement in CPMV entry, due to relatively small effect of inhibitors of clathrin-mediated endocytosis, and the exclusion of CPMV particles from early (EEA1) endosomes associated with clathrin-mediated endocytosis. The roles of both caveolae-mediated endocytosis and macropinocytosis in CPMV internalization were identified based on specific inhibitor and colocalization studies. Our studies suggest that CPMV entry occurs via multiple pathways including caveolae and macropinocytosis, and travels through Rab5+ early endosomes, en route to a lysosomal compartment, with some particles trafficking through recycling Rab11+ endosomes and possibly back to the cell surface. This recycling pathway may be potentially used for the display of surface vimentin on cells as well.

Entry by caveolae is dependent on cholesterol, and the inhibitors nystatin and filipin III are highly selective inhibitors that sequester cholesterol and other lipids from cell membranes³⁹. When cells were treated with these inhibitors of caveolae formation, nanoparticle uptake was reduced, although not completely eliminated. These results are consistent with studies of *E.coli* Ibe-A mediated invasion of endothelial cells, a pathogen that also uses surface vimentin as a cell binding protein. Ibe-A mediated entry via vimentin is thought to occur via caveolae, as filipinIII and nystatin each inhibited IbeA-mediated invasion⁴⁰.

Macropinocytosis incorporates lipid rafts as well. When specific inhibitors of macropinocytosis were utilized, CPMV uptake was also partially reduced. In addition, CPMV demonstrated some colocalization with the fluid phase marker FITC-dextran (Figure 3D and E), further supporting the involvement of macropinocytosis in CPMV entry.

The study of viral nanoparticle entry differs from previous virus entry studies that have focused on replicating viruses⁴¹. Upon entering a host cell that is permissive to infection, a virus typically initiates the process of replication. This process produces expansion of viral

gene and protein products including synthesis of viral RNA and proteins, and the production of exponential increases in the numbers of virus particles. These readouts provide a magnified output that allows for sensitive measurement and quantification when perturbing virus entry pathways by genetic or chemical means. In the case of CPMV, which readily enters but to our knowledge does not replicate in mammalian cells, these measures of replication are not available. Because of this limitation, studies of nanoparticle uptake necessitate the use of relatively large amounts of particles to ensure detection of the particles. Thus while both caveolae and macropinocytosis were shown to play a role in CPMV entry, one or the other pathway may be favored when lower ratios of CPMV particles:cell are present.

Many viruses often utilize multiple pathways for entry. When the readout of entry is the product of replication, the investigation is focused on the productive route of entry. In this case, even though virus particles are entering by multiple routes, one only measures the productive route of entry. For example, although infection by Bluetongue virus was previously thought to be clathrin-dependent⁴², studies have subsequently shown a strong involvement of a pathway that is similar to macropinocytosis⁴³. Endocytic pathways have been identified for a variety of other non-viral nanoparticle formulations, and in many cases the studies demonstrate the involvement of multiple endocytic pathways. In the case of a synthetic nanoparticle, hydrophobically modified glycol chitosans, each of the major pathways of endocytosis was determined to be involved with entry. Clathrin- and caveolae-mediated endocytosis and macropinocytosis inhibitors were each shown to reduce uptake of these particle to a degree, resulting in the conclusion that each pathway was partially involved⁴⁴. In the case of quantum dots targeted for endocytic release with nona-arginine cell-penetrating peptide, the macropinocytosis pathway showed the most significant involvement, and yet investigations into clathrin- and caveolin-mediated pathways failed to completely rule them out⁴⁵. Pharmacologic inhibitors of endocytosis are also known to have some overlap between endocytic pathways. Because CPMV entry was not blocked completely by caveolae inhibitors, future studies inhibiting caveolin-1 expression with siRNA or shRNA may be informative. A similar experiment utilizing siRNA to knock down expression of clathrin heavy chain in cells could further rule out the potential for involvement of clathrin in CPMV entry. Because several pathways are involved, it is also possible that combinations of inhibitors could further illuminate the players in CPMV internalization. It will also be important to study the internalization mechanism in additional cell types important for CPMV targeting *in vivo* including endothelial cells, central nervous system inflammatory cells, and macrophage sub-populations^{3, 9, 33, 46}.

As the use of nanoparticles for imaging and therapeutic applications increases, so too does our need to understand the route of entry in order to improve their effectiveness. The route of entry may affect not only the particle formulation but the types of cargo being encapsidated as well, since changes in endosome pH or the presence of endosomal proteases may influence the activity of the cargo upon release. Further studies of the entry mechanism of CPMV both non-targeted and targeted to specific cell-surface receptors may provide clues as to the most efficient routes of entry that are associated with optimal intracellular localization and delivery.

Supplementary Material

Refer to Web version on PubMed Central for supplementary material.

Acknowledgments

We would like to acknowledge the UCSD Neuroscience Microscopy facility, Grant P30 NS047101. This work was supported by National Institutes of Health R01CA112075 (M.M.), and grants from the American Heart Association to E.M.P. and to M.M.

Abbreviations

CPMV Cowpea mosaic virus

References

1. Plummer EM, Manchester M. Viral nanoparticles and virus-like particles: platforms for contemporary vaccine design. *Wiley Interdiscip Rev Nanomed Nanobiotechnol*.
2. Pokorski JK, Steinmetz NF. The art of engineering viral nanoparticles. *Mol Pharm*. 8(1):29–43. [PubMed: 21047140]
3. Lewis JD, Destito G, Zijlstra A, Gonzalez MJ, Quigley JP, Manchester M, Stuhlmann H. Viral nanoparticles as tools for intravital vascular imaging. *Nat Med*. 2006; 12(3):354–360. [PubMed: 16501571]
4. Muldoon LL, Nilaver G, Kroll RA, Pagel MA, Breakefield XO, Chiocca EA, Davidson BL, Weissleder R, Neuwelt EA. Comparison of intracerebral inoculation and osmotic blood-brain barrier disruption for delivery of adenovirus, herpesvirus, and iron oxide particles to normal rat brain. *Am J Pathol*. 1995; 147(6):1840–1851. [PubMed: 7495307]
5. Raty JK, Liimatainen T, Wirth T, Airene KJ, Ihalainen TO, Huhtala T, Hamerlynck E, Vihinen-Ranta M, Narvanen A, Yla-Herttuala S, Hakumaki JM. Magnetic resonance imaging of viral particle biodistribution in vivo. *Gene Ther*. 2006; 13(20):1440–1446. [PubMed: 16855615]
6. Singh P, Prasuhn D, Yeh RM, Destito G, Rae CS, Osborn K, Finn MG, Manchester M. Biodistribution, toxicity and pathology of cowpea mosaic virus nanoparticles in vivo. *J Control Release*. 2007; 120(1–2):41–50. [PubMed: 17512998]
7. Rae CS, Khor IW, Wang Q, Destito G, Gonzalez MJ, Singh P, Thomas DM, Estrada MN, Powell E, Finn MG, Manchester M. Systemic trafficking of plant virus nanoparticles in mice via the oral route. *Virology*. 2005; 343(2):224–235. [PubMed: 16185741]
8. Leong HS, Steinmetz NF, Ablack A, Destito G, Zijlstra A, Stuhlmann H, Manchester M, Lewis JD. Intravital imaging of embryonic and tumor neovasculature using viral nanoparticles. *Nat Protoc*. 5(8):1406–1417. [PubMed: 20671724]
9. Shriver LP, Koudelka KJ, Manchester M. Viral nanoparticles associate with regions of inflammation and blood brain barrier disruption during CNS infection. *J Neuroimmunol*. 2009; 211(1–2):66–72. [PubMed: 19394707]
10. Plummer EM, Thomas D, Destito G, Shriver LP, Manchester M. Interaction of cowpea mosaic virus nanoparticles with surface vimentin and inflammatory cells in atherosclerotic lesions. *Nanomedicine (Lond)*.
11. Koudelka KJ, Destito G, Plummer EM, Trauger SA, Siuzdak G, Manchester M. Endothelial targeting of cowpea mosaic virus (CPMV) via surface vimentin. *PLoS Pathog*. 2009; 5(5) e1000417.
12. Koudelka KJ, Rae CS, Gonzalez MJ, Manchester M. Interaction between a 54-kilodalton mammalian cell surface protein and cowpea mosaic virus. *J Virol*. 2007; 81(4):1632–1640. [PubMed: 17121801]
13. Mor-Vaknin N, Punturieri A, Sitwala K, Markovitz DM. Vimentin is secreted by activated macrophages. *Nat Cell Biol*. 2003; 5(1):59–63. [PubMed: 12483219]
14. Podor TJ, Singh D, Chindemi P, Foulon DM, McKelvie R, Weitz JI, Austin R, Boudreau G, Davies R. Vimentin exposed on activated platelets and platelet microparticles localizes vitronectin and plasminogen activator inhibitor complexes on their surface. *J Biol Chem*. 2002; 277(9):7529–7539. [PubMed: 11744725]

15. Xu B, deWaal RM, Mor-Vaknin N, Hibbard C, Markovitz DM, Kahn ML. The endothelial cell-specific antibody PAL-E identifies a secreted form of vimentin in the blood vasculature. *Mol Cell Biol.* 2004; 24(20):9198–9206. [PubMed: 15456890]
16. Bryant AE, Bayer CR, Huntington JD, Stevens DL. Group A streptococcal myonecrosis: increased vimentin expression after skeletal-muscle injury mediates the binding of *Streptococcus pyogenes*. *J Infect Dis.* 2006; 193(12):1685–1692. [PubMed: 16703512]
17. Steinmetz NF, Cho CF, Ablack A, Lewis JD, Manchester M. Cowpea mosaic virus nanoparticles target surface vimentin on cancer cells. *Nanomedicine (Lond).* 6(2):351–364. [PubMed: 21385137]
18. Hajitou A, Pasqualini R, Arap W. Vascular targeting: recent advances and therapeutic perspectives. *Trends in cardiovascular medicine.* 2006; 16(3):80–88. [PubMed: 16546688]
19. Ruoslahti E. Specialization of tumour vasculature. *Nat Rev Cancer.* 2002; 2(2):83–90. [PubMed: 12635171]
20. Nanda A, St. Croix B. Tumor endothelial markers: new targets for cancer therapy. *Currnt Opinion Oncology.* 2004; 16:44–49.
21. Sugahara KN, Teesalu T, Karmali PP, Kotamraju VR, Agemy L, Girard OM, Hanahan D, Mattrey RF, Ruoslahti E. Tissue-penetrating delivery of compounds and nanoparticles into tumors. *Cancer cell.* 2009; 16(6):510–520. [PubMed: 19962669]
22. Rajendran L, Knolker HJ, Simons K. Subcellular targeting strategies for drug design and delivery. *Nat Rev Drug Discov.* 2010; 9(1):29–42. [PubMed: 20043027]
23. Huth US, Schubert R, Peschka-Suss R. Investigating the uptake and intracellular fate of pH-sensitive liposomes by flow cytometry and spectral bio-imaging. *J Control Release.* 2006; 110(3):490–504. [PubMed: 16387383]
24. Kee SH, Cho EJ, Song JW, Park KS, Baek LJ, Song KJ. Effects of endocytosis inhibitory drugs on rubella virus entry into VeroE6 cells. *Microbiology and immunology.* 2004; 48(11):823–829. [PubMed: 15557740]
25. Rajendran L, Knolker HJ, Simons K. Subcellular targeting strategies for drug design and delivery. *Nat Rev Drug Discov.* 9(1):29–42. [PubMed: 20043027]
26. Mudhakir D, Harashima H. Learning from the viral journey: how to enter cells and how to overcome intracellular barriers to reach the nucleus. *The AAPS journal.* 2009; 11(1):65–77. [PubMed: 19194803]
27. Dessens JT, Lomonossoff GP. Cauliflower mosaic virus 35S promoter-controlled DNA copies of cowpea mosaic virus RNAs are infectious on plants. *J Gen Virol.* 1993; 74(Pt 5):889–892. [PubMed: 8492093]
28. Siler DJ, Babcock J, Bruening G. Electrophoretic mobility and enhanced infectivity of a mutant of cowpea mosaic virus. *Virology.* 1976; 71(2):560–567. [PubMed: 936474]
29. Wang Q, Kaltgrad E, Lin T, Johnson JE, Finn MG. Natural supramolecular building blocks. Wild-type cowpea mosaic virus. *Chem Biol.* 2002; 9(7):805–811. [PubMed: 12144924]
30. Thompson HM, McNiven MA. Discovery of a new 'dynasore'. *Nat Chem Biol.* 2006; 2(7):355–356. [PubMed: 16783339]
31. Destito G, Yeh R, Rae CS, Finn MG, Manchester M. Folic acid-mediated targeting of cowpea mosaic virus particles to tumor cells. *Chem Biol.* 2007; 14(10):1152–1162. [PubMed: 17961827]
32. Wu Z, Chen K, Yildiz I, Dirksen A, Fischer R, Dawson PE, Steinmetz NF. Development of viral nanoparticles for efficient intracellular delivery. *Nanoscale.*
33. Gonzalez MJ, Plummer EM, Rae CS, Manchester M. Interaction of Cowpea mosaic virus (CPMV) nanoparticles with antigen presenting cells in vitro and in vivo. *PLoS One.* 2009; 4(11):e7981. [PubMed: 19956734]
34. Ivanov AI. Pharmacological inhibition of endocytic pathways: is it specific enough to be useful? *Methods Mol Biol.* 2008; 440:15–33. [PubMed: 18369934]
35. Wang LH, Rothberg KG, Anderson RG. Mis-assembly of clathrin lattices on endosomes reveals a regulatory switch for coated pit formation. *J Cell Biol.* 1993; 123(5):1107–1117. [PubMed: 8245121]
36. Beignon AS, McKenna K, Skoberne M, Manches O, DaSilva I, Kavanagh DG, Larsson M, Gorelick RJ, Lifson JD, Bhardwaj N. Endocytosis of HIV-1 activates plasmacytoid dendritic cells

- via Toll-like receptor-viral RNA interactions. *J Clin Invest.* 2005; 115(11):3265–3275. [PubMed: 16224540]
37. Parton RG, Simons K. The multiple faces of caveolae. *Nat Rev Mol Cell Biol.* 2007; 8(3):185–194. [PubMed: 17318224]
38. Rubino M, Miaczynska M, Lippe R, Zerial M. Selective membrane recruitment of EEA1 suggests a role in directional transport of clathrin-coated vesicles to early endosomes. *J Biol Chem.* 2000; 275(6):3745–3748. [PubMed: 10660521]
39. Ros-Baro A, Lopez-Iglesias C, Peiro S, Bellido D, Palacin M, Zorzano A, Camps M. Lipid rafts are required for GLUT4 internalization in adipose cells. *Proc Natl Acad Sci U S A.* 2001; 98(21): 12050–12055. [PubMed: 11593015]
40. Chi F, Jong TD, Wang L, Ouyang Y, Wu C, Li W, Huang SH. Vimentin-mediated signalling is required for IbeA+ *E. coli* K1 invasion of human brain microvascular endothelial cells. *Biochem J.* 427(1):79–90. [PubMed: 20088823]
41. Mercer J, Schelhaas M, Helenius A. Virus entry by endocytosis. *Annu Rev Biochem.* 79:803–833. [PubMed: 20196649]
42. Forzan M, Marsh M, Roy P. Bluetongue virus entry into cells. *J Virol.* 2007; 81(9):4819–4827. [PubMed: 17267479]
43. Gold S, Monaghan P, Mertens P, Jackson T. A clathrin independent macropinocytosis-like entry mechanism used by bluetongue virus-1 during infection of BHK cells. *PLoS One.* 5(6):e11360. [PubMed: 20613878]
44. Nam HY, Kwon SM, Chung H, Lee SY, Kwon SH, Jeon H, Kim Y, Park JH, Kim J, Her S, Oh YK, Kwon IC, Kim K, Jeong SY. Cellular uptake mechanism and intracellular fate of hydrophobically modified glycol chitosan nanoparticles. *J Control Release.* 2009; 135(3):259–267. [PubMed: 19331853]
45. Xu Y, Liu BR, Lee HJ, Shannon KB, Winiarz JG, Wang TC, Chiang HJ, Huang YW. Non-arginine facilitates delivery of quantum dots into cells via multiple pathways. *J Biomed Biotechnol.* 2010 948543.
46. Plummer EM, Thomas D, Destito G, Shriver LP, Manchester M. Interaction of cowpea mosaic virus nanoparticles with surface vimentin and inflammatory cells in atherosclerotic lesions. *Nanomedicine (Lond).* 7(6):877–888. [PubMed: 22394183]

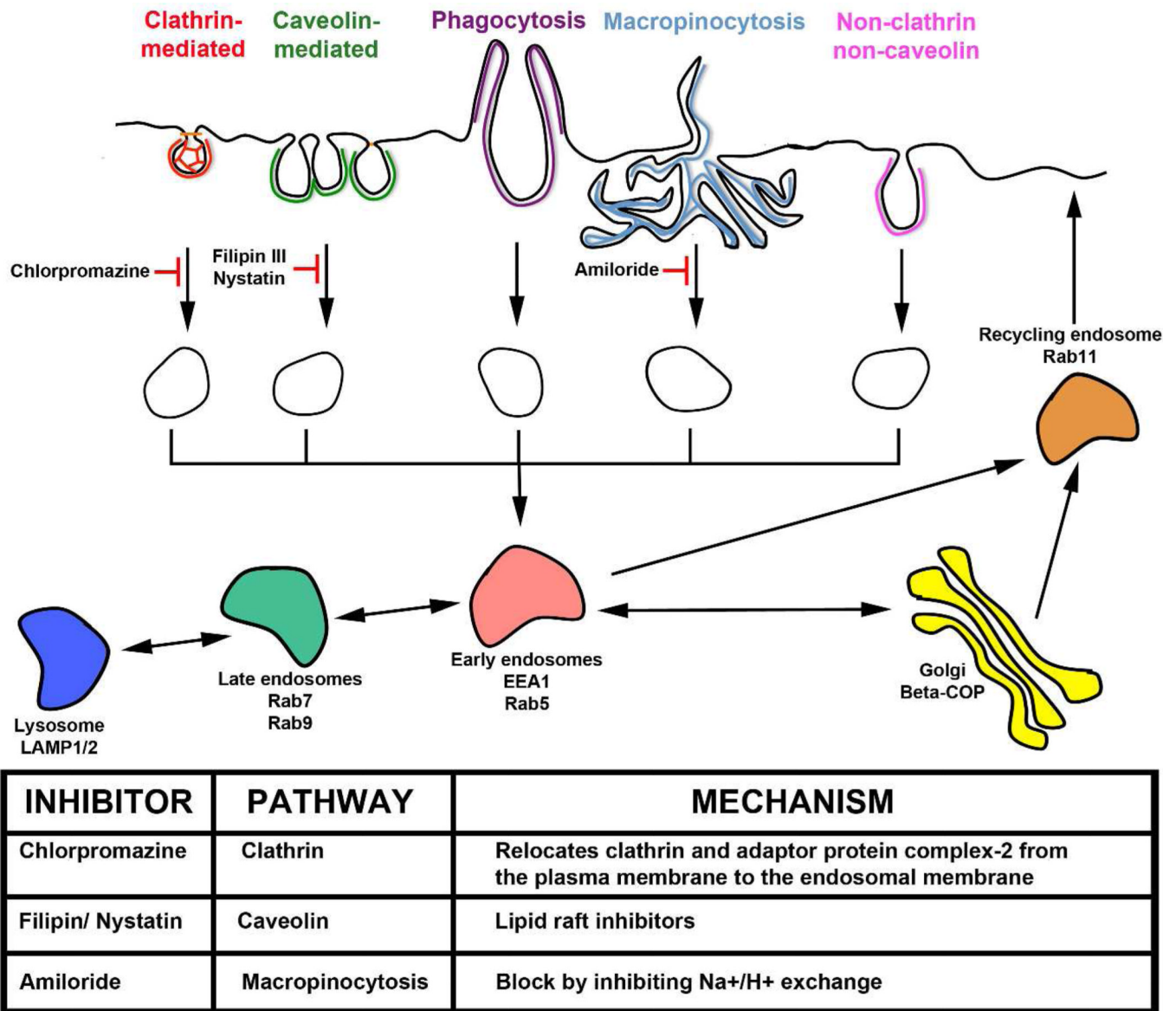


Figure 1. Routes, markers, and Inhibitors of endocytic pathways

Classical routes of endocytosis are shown across the top and their inhibitors are shown below with their effect on each pathway (solid line - confirmed inhibition; dotted line - possible/partial inhibition). Chlorpromazine inhibits internalization involving clathrin., Filipin III and Nystatin block internalization by caveolae. Amiloride inhibits macropinocytosis. Markers of early endosomes are in red (EEA1) and blue (Rab5). Markers of late endosome/lysosome (Rab9, LAMP-2) are in green and orange. Markers of recycling endosome (Rab11) are in purple. Adapted from Rajendran et al.²⁵.

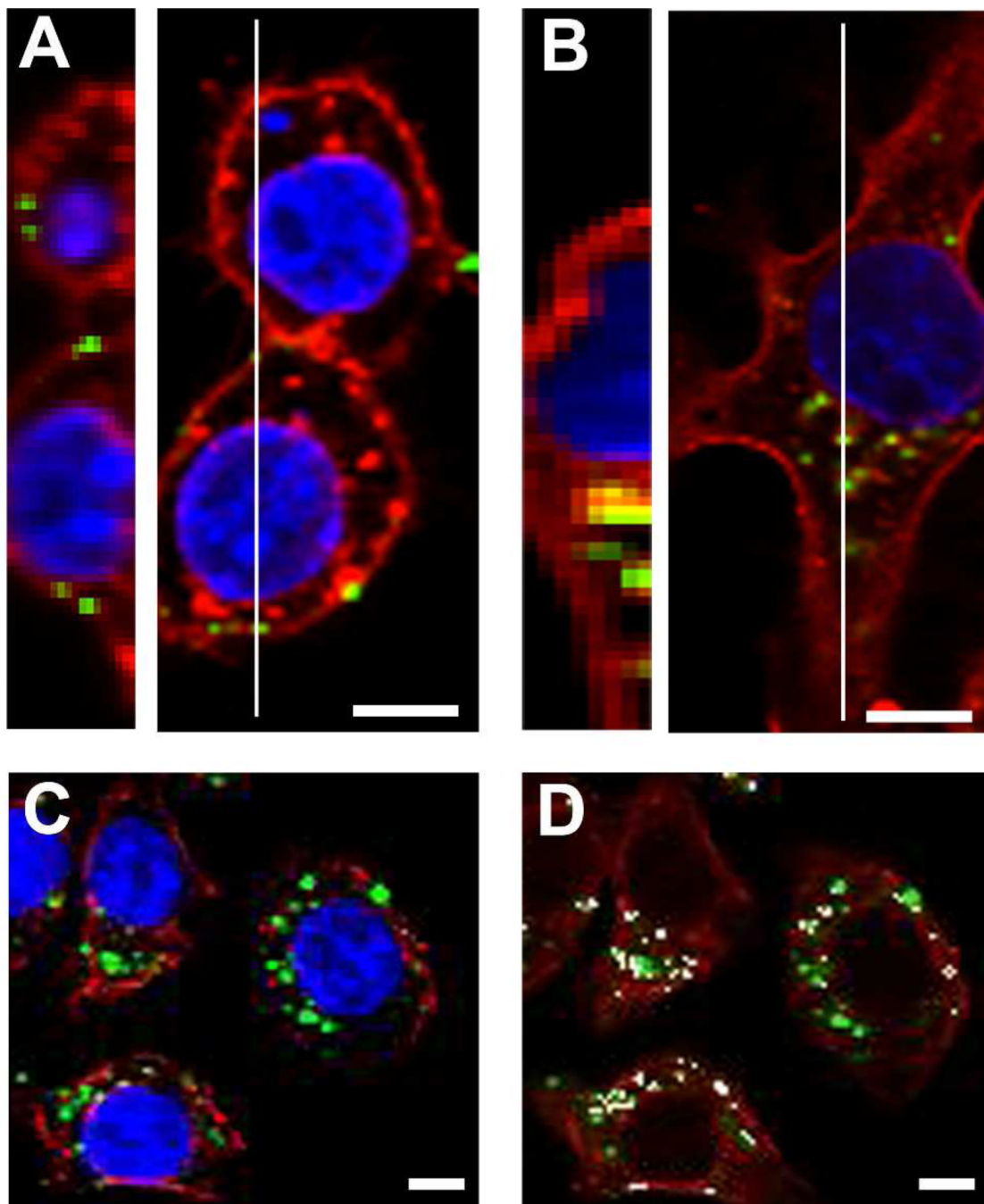


Figure 2. CPMV is bound and internalized by RAW264.7 macrophages and accumulates in late endosomes

(A) CPMV-AF647 was incubated with RAW264.7 macrophages for one hour at 4 °C with 1×10^6 viruses/cell. (B) CPMV-AF647 was incubated with RAW264.7 macrophages for four hours at 37 °C with 1×10^6 viruses/cell. Slices through cells were imaged by confocal microscopy and multiple slices in a Z-series at the white line in left images and were compiled using ImageJ to make images on right. Bar, 5 μ m. (C–D) RAW264.7 macrophages were incubated with CPMV-AF647 for four hours at 37 °C. Confocal microscopy imaging revealed colocalization (white, D) of CPMV fluorescence (green) and fluorescent antibody staining of LAMP-2 (red).

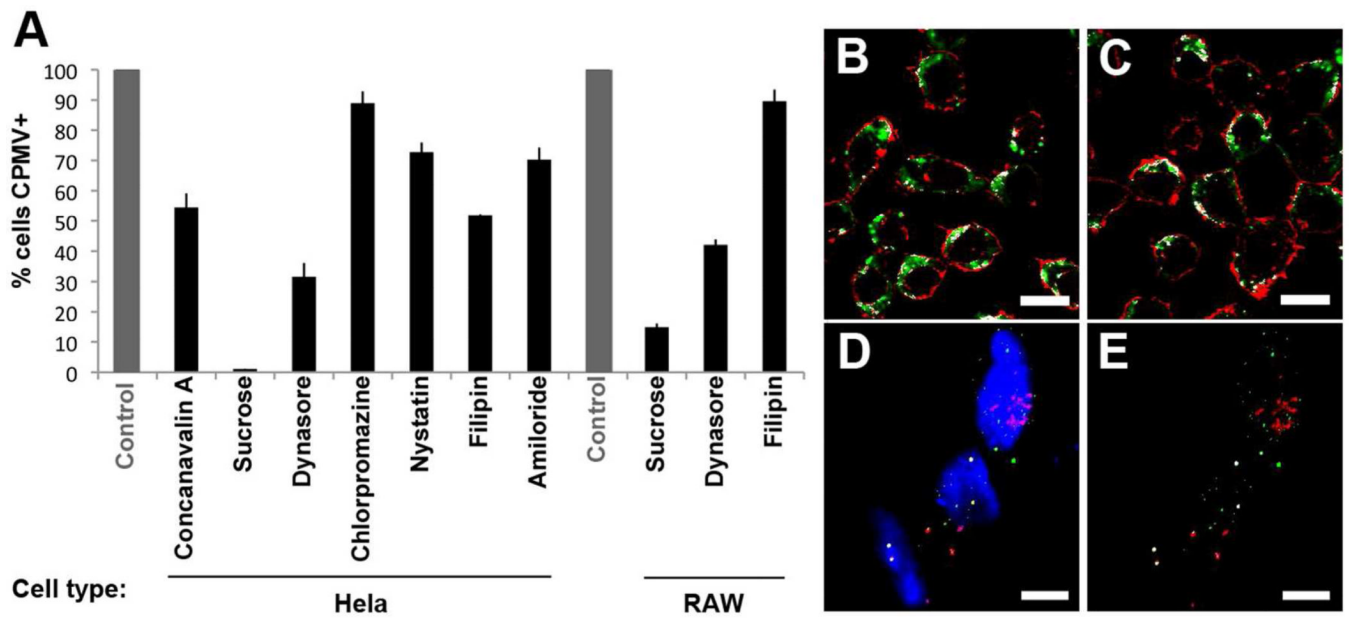


Figure 3. Reduction of CPMV endocytosis under nonspecific and specific inhibitors

Hela and RAW264.7 cells were treated with endocytic inhibitors and incubated with fluorescently-labeled CPMV. Flow cytometry was used to confirm the change in CPMV endocytosis. All controls without inhibitors were normalized to 100% uptake. The effects of nonspecific (concanavalin A, hypertonic sucrose) and specific inhibitors targeting clathrin (chlorpromazine), caveolae (nystatin and filipin), dynamin (dynasore) and macropinocytosis (MPC, amiloride) are shown. ImageJ analysis of the percent colocalization of CPMV with the cell surface stain wheat germ agglutinin in RAW264.7 macrophages. Representative images show the colocalization (white) of CPMV (green) with membrane surface stain (red) under normal (B) and dynamin inhibition conditions (C). (D–E) Confocal image of CPMV (green) and internalizing fluid phase marker FITC-dextran (E) and their colocalization in white (F). Bar, 10 μ m.

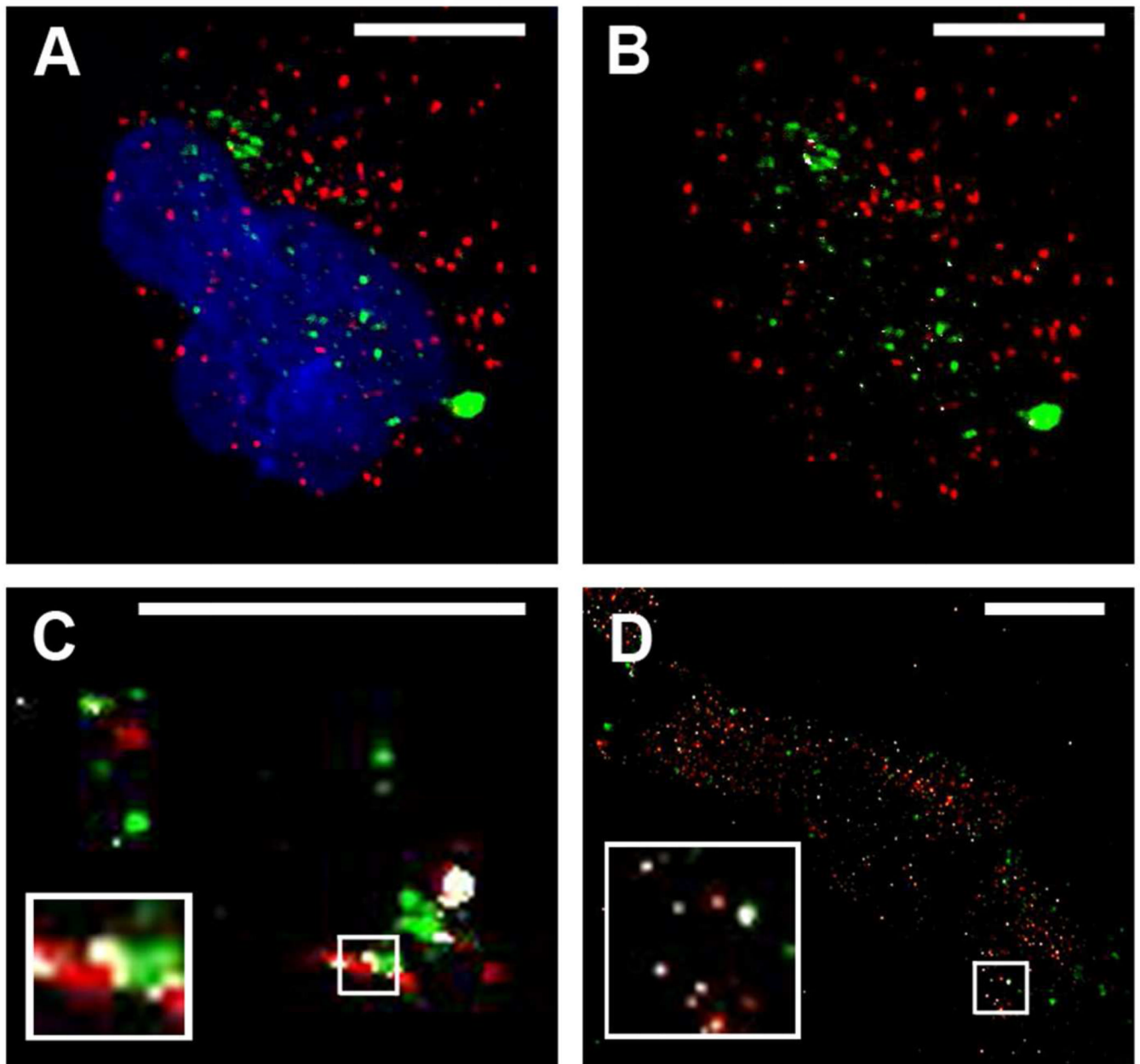


Figure 4. Determining localization of CPMV with endosomal markers EEA1, Rab 5, and Rab 11 (A–B) HeLa cells incubated 2 hr with CPMV (green) and stained for EEA1 (red). White in B shows colocalized points. Amount of colocalization representative of all timepoints studies (30 min, 1 hr, 2 hr, and 4 hr). (C) Partial colocalization of internalizing CPMV with early endosomal marker Rab5. RAW264.7 macrophages incubated with CPMV (green) for 45 minutes and stained with Rab5 antibody (red). This timepoint showed the most colocalization (white, compared with 15, 30, and 60 minutes). (D) Partial colocalization of internalizing CPMV with recycling endosome marker Rab11. HeLa cells were incubated with CPMV (green) for 3 hrs and stained with Rab11. Bar, 10 μ m.